JACS
JOURNAL OF THE AMERICAN CHEMICAL SOCIETY

COMMUNICATION

pubs.acs.org/JACS

Regioregular Pyridal[2,1,3]thiadiazole π-Conjugated Copolymers

Lei Ying,[†] Ben B. Y. Hsu,[†] Hongmei Zhan,[†,‡] Gregory C. Welch,[†] Peter Zalar,[†] Louis A. Perez,[†] Edward J. Kramer,[†] Thuc-Quyen Nguyen,[†] Alan J. Heeger,[†] Wai-Yeung Wong,[‡] and Guillermo C. Bazan*[,†]

[†]Center for Polymers and Organic Solids, Departments of Chemistry & Biochemistry and Materials, University of California, Santa Barbara, California 93106, United States

[‡]Institute of Molecular Functional Materials and Department of Chemistry and Centre for Advanced Luminescence Materials, Hong Kong Baptist University, Waterloo Road, Hong Kong, P.R. China

Supporting Information

ABSTRACT: π-Conjugated, narrow band gap copolymers containing pyridal[2,1,3]thiadiazole (PT) were synthesized via starting materials that prevent random incorporation of the PT heterocycles relative to the backbone vector. Two regioregular structures could be obtained: in one the PTs are oriented in the same direction, and in the other the orientation of the PTs alternates every other repeat unit. Compared to their regiorandom counterparts, the regioregular polymers exhibit a 2 orders of magnitude increase of the hole mobilites, from 0.005 to 0.6 $cm^2\ V^{-1}\ s^{-1}$, as determined by field-effect transistor measurements.

Narrow band gap π-conjugated copolymers comprised of electron-rich (donor) and -poor (acceptor) moieties give rise to broad intramolecular charge-transfer excitations that can be tuned to match the solar spectrum and can organize in the solid state so that suitably high charge carrier mobilities can be achieved.[1,2] A well-appreciated class of polymers incorporates cyclopenta[2,1-*b*:3,4-*b*′]dithiophene (CDT) and 2,1,3-benzothiadiazole (BT) comonomers.[3] More recently, the pyridal[2,1,3]-thiadiazole (PT) acceptor has been used instead of BT; this modification results in higher electron affinity in the backbone and leads to narrower optical gaps.[4] It should be noted, however, that the N (PT) for C−H (BT) substitution also reduces the symmetry of the repeat unit.

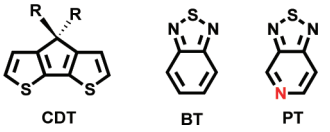

Regioregular conjugated polymers exhibit better π-stacking than their regiorandom counterparts.[5,6] A classic example involves regioregular poly(3-alkylthiophene), for which higher crystallinity, red-shifted optical absorption, and larger charge carrier mobilities are observed when the monomers are arranged in a head-to-tail configuration.[6] Other polymer architectures exist, such as poly(2,5-bis(3-alkylthiophen-2-yl)thieno[3,2-*b*]thiophene) (pBTTT), in which centrosymmetric comonomer units naturally lead to symmetric backbone structures and thereby alleviate synthetic concerns.[7]

It seemed reasonable that similar structural considerations should apply to PT-containing polymers. As shown in Scheme 1, alternating copolymers containing PT may exhibit two possible regioregular structures. In type I, the PT heterocycles are positioned along the chain vector so that the pyridal nitrogens point in same direction. Type II illustrates the situation when the PT heterocycles alternate in orientation. One outcome from these considerations is that type I contains a smaller repeat unit, defined here as the chemical entity with which translational symmetry can describe the entire chain. In this contribution, we provide synthetic strategies for accessing PT-containing polymers of types I and II and show that these materials have considerably higher charge carrier mobilities relative to those obtained using conventional condensation polymerization procedures.

Scheme 1. Regiochemically Precise PT-Containing Alternating Copolymer Structures[a]

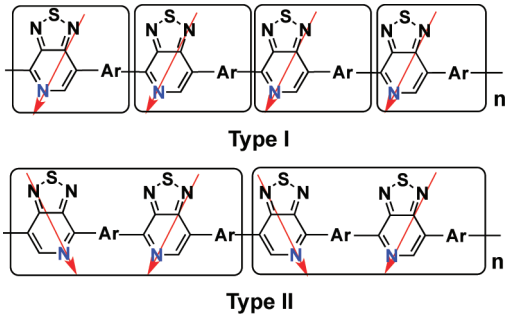

[a] Ar corresponds to a symmetric π-conjugated structural unit. The arrows indicate the difference in heterocycle orientation.

Our synthetic approach to regioregular PT-containing polymers is centered on the chemistry of 4,7-dibromo[1,2,5]thiadiazolo[3,4-*c*]-pyridine ($PTBr_2$). On the basis of the reactivity of 2,5-dibromopyridine, it was anticipated that Pd-mediated cross-coupling of $PTBr_2$ with stannylated aromatic compounds would preferentially occur at C−Br adjacent to the pyridal N atom.[8] Scheme 2a shows how this reactivity can be used to synthesize poly[4-(4,4-dihexadecyl-4*H*-cyclopenta[1,2-*b*:5,4-*b*′]dithiophen-2-yl)-*alt*-[1,2,5]-thiadiazolo[3,4-*c*]pyridine] of type I, i.e., **P1**. Microwave-assisted crosscoupling of (4,4-dihexadecyl-4*H*-cyclopenta[1,2-*b*:5,4*b*′]dithiophen-2-yl)trimethylstannane (**M1**) and $PTBr_2$ in the presence of $Pd(PPh_3)_4$ affords CDT-PT-Br (**M2**) in yields as high as 90%. The proposed regiochemistry was confirmed by $^1H-^1H$ NOE spectroscopy (Figure S1 in the Supporting

Received: August 10, 2011
Published: September 21, 2011

Scheme 2. Synthesis of P1, P2, and P3

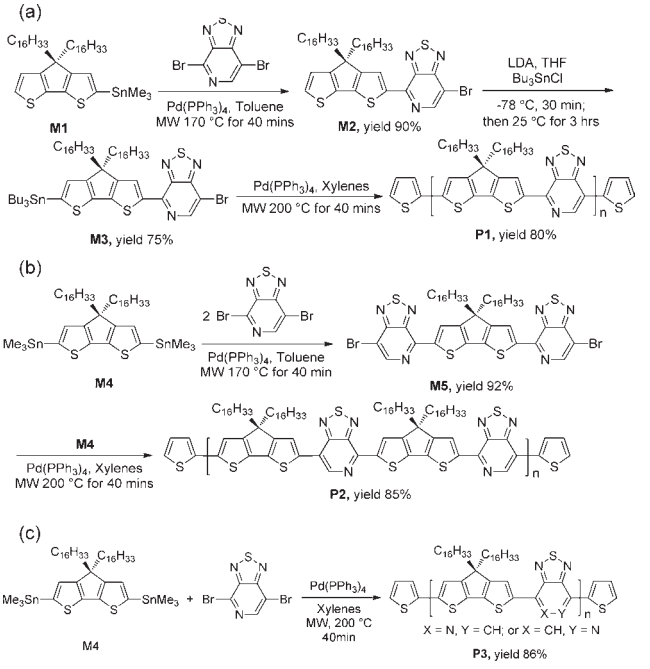

Information (SI)), where no cross-correlation peaks can be observed between CDT and PT proton resonances.[4e] Treatment of **M2** with lithium diisopropylamide (LDA), followed by quenching with tributylstannyl chloride (Bu_3SnCl), gave Bu_3Sn-CDT-PT-Br (**M3**) in 75% yield. Polymerization of **M3** using $Ph(PPh_3)_4$ as the catalyst in xylenes afforded **P1**. The fact that the two reactive functional groups involved in the polymerization sequence are introduced within a single precursor ensures strict alignment of structural units along the polymer. All the polymers described here were capped with thiophene units to minimize residual Br and Sn terminal groups.[9]

A different approach was required to prepare an analogous polymer of type II. The building block requires an aromatic subunit in which two pyridal nitrogens are oriented toward a central CDT fragment. As shown in Scheme 2b, reaction of (4,4-dihexadecyl-4*H*-cyclopenta[1,2-*b*:5,4-*b*′]dithiophene-2,6-diyl)bis(trimethylstannane) (**M4**) with $PTBr_2$ yields the target compound Br-PT-CDT-PT-Br (**M5**). Note the high yield of the reaction (92%) and that a perpendicular plane of symmetry in **M5** bisects the cyclopentadienyl core and contains the two α-carbons in the alkyl chains. Polymerization of **M4** and **M5** gave the regioregular copolymer **P2**.

As shown in Scheme 2c, the PT-CDT copolymer **P3** was prepared by using a standard one-pot polymerization involving **M4** and $PTBr_2$. Given the regioselectivity of the reaction between $PTBr_2$ and stannylated species, one may anticipate some bias in the structure of **P3**; however, it is unlikely to be as perfect as that achieved with **P1** and **P2**. Indeed, characterization of the polymers by NMR spectroscopy shows this to be the case, as discussed in more detail below.

Polymers **P1**−**P3** are poorly soluble in common organic solvents. Two batches of different molecular weights were prepared for each type by controlling the reaction conditions. Low molecular weight **P1** (M_n = 8 kDa, ~10 repeat units, polydispersity (PDI) = 1.9) was prepared by adding the catalyst under air before the microwave tube was sealed for polymerization. **P2** (M_n = 15 kDa, PDI = 1.9) and **P3** (M_n = 12 kDa, PDI = 2.2) were prepared by

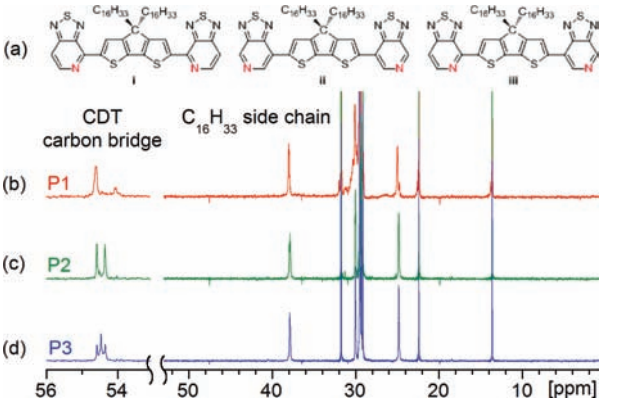

Figure 1. (a) Molecular structures of PT-CDT-PT moieties, and ^{13}C NMR spectra in *o*-DCB-d_4 at 110 °C for (b) **P1**, (c) **P2**, and (d) **P3**.

adding 10 mol % excess **M4** in the polymerization reaction. The more soluble, lower molecular weight samples were used for solution NMR characterization. Charge carrier mobilities (described in more detail below) were determined with samples of higher molecular weight (**P1**, M_n = 28 kDa, PDI = 1.9; **P2**, M_n = 34 kDa, PDI = 3.1; **P3**, M_n = 40 kDa, PDI = 2.5). Analysis of all the samples by standard differential scanning calorimetry revealed no distinct phase transition upon heating up to 300 °C (Figure S2).

Insight into the polymer regiochemistry was obtained by NMR analysis of the low molecular weight samples. Peaks in the ^1H NMR spectra proved too broad and lacked a sufficient range of chemical shifts for differentiation (Figure S3). However, as shown in Figure 1, the ^{13}C NMR signals from the dithiophene bridge carbon (C_{CDT}) proved diagnostic. Consideration of the structure led us to anticipate three unique signals, denoted as **i**, **ii**, and **iii** in Figure 1a, assuming that the chemical shifts are determined predominantly by the relative positions of adjacent PT units. A single resonance for C_{CDT}, corresponding to structure **iii**, should be observed if **P1** is described by a type I structure. Indeed, as shown in Figure 1b, one signal at 54.6 ppm dominates the spectrum; we attribute the smaller contribution at 54.1 ppm to end group contributions. Note that the average degree of polymerization is consistent with the ratio of integrated signals (10:1). Two signals, from structures **i** and **ii**, would be indicative of structure **P2**. The peaks at 54.6 and 54.4 ppm in Figure 1c show that this is the case, although it is not possible to make unambiguous assignments. Less precision would be expected for **P3**; its ^{13}C NMR spectrum in Figure 1d reveals three peaks (54.6, 54.5, and 54.4 ppm), which can be reasonably accounted for by a statistical contribution from the three possible substructures **i**, **ii**, and **iii**. Overall, these data are consistent with the proposed regioregular structures of **P1** and **P2** and reveal that a considerably less precise arrangement of comonomer units is obtained via the standard protocol in Scheme 2c.

Solution and thin-film UV−vis−near-infrared absorption spectra of **P1**, **P2**, and **P3** are presented in Figure 2. With the samples both in 1,2-dichlorobenzene (*o*-DCB) solutions at 25 °C and as thin films, the maximum absorption (λ_{max}) exhibits a gradual bathochromic shift from 880 nm for random **P3**, to 885 nm for **P2**, and 930 nm for **P1**. No distinct red shift in λ_{max} is observed for all three polymers after transitioning to the solid state. In comparison to the solution at 25 °C, heating the *o*-DCB solutions to 110 °C reveals hypsochromic shifts to 810 nm for **P1**, 805 nm for **P2**, and 800 nm for **P3**, which suggest breakup of aggregated chains (Figure S4).[10] The optical band gaps

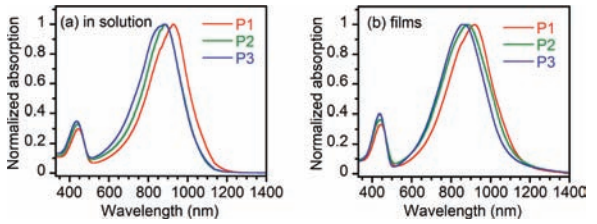

Figure 2. Absorption spectra of **P1**, **P2**, and **P3** (1.0×10^{-5} g/mL) at 25 °C in *o*-DCB (a) and as thin films (b).

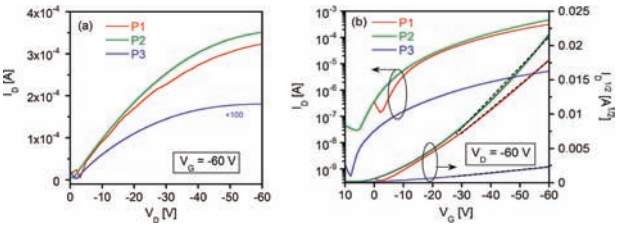

Figure 3. FET characteristics of **P1**, **P2**, and **P3** spin-coated on OTS8-treated SiO_2/Si substrates (L = 20 μm, W = 1 mm): (a) output curves taken at $V_G = -60$ V, curve for **P3** was the result multiplied by 100; (b) transfer curves displaying the saturation regime with $V_D = -60$ V. The mobility values were calculated from the dashed lines in panel b.

Table 1. CV, Photophysical, and FET Measurements of P1−P3

polymer	P1	P2	P3
E_{HOMO}/E_{LUMO}[a] [eV]	−5.07/−3.70	−5.16/−3.70	−5.23/−3.69
E_g^{cvb}[b] [eV]	1.37	1.46	1.54
$\lambda_{max}^{sol}/\lambda_{max}^{filmsc}$ [nm]	930/920	885/885	880/870
E_g^{optd}[d] [eV]	1.09	1.12	1.15
μ_{sat}[e] [$cm^2\ V^{-1}\ s^{-1}$]	0.4 (0.3)	0.6 (0.5)	0.005 (0.005)
I_{on}/I_{off}	2×10^3	2×10^4	1×10^4

[a] Highest occupied molecular orbital energy level calculated from the onset of oxidation, and lowest unoccupied molecular orbital energy level calculated from the onset of reduction. [b] Energy band gap calculated from the difference between E_{HOMO} and E_{LUMO}. [c] Maximum absorption at 25 °C in *o*-DCB and in films. [d] Energy band gap calculated from the onset of film absorption band. [e] Highest FET hole mobilities in the saturation regime; average values based on 20 devices are shown in parentheses.

determined by the absorption onset in films are 1.09−1.15 eV. Altogether, these data indicate that regioregularity decreases the band gap of the polymers; however, it is unclear at this stage whether this change is due to increased delocalization, i.e., improved coplanarity of the repeat units, or to effects associated with the influence of organized dipoles on the efficiency of charge transfer among the donor and acceptor substructures.

Cyclic voltammetry (CV) measurements were carried out to probe the influence of polymer structure on the frontier molecular orbitals.[11] A summary of the results is in Table 1; full details can be found in the SI (Figure S5 and Table S2). **P1**−**P3** exhibit similar lowest unoccupied molecular orbital (LUMO) energy levels ($E_{LUMO} \approx -3.7$ eV), because E_{LUMO} of such donor−acceptor copolymers mainly resides on the electron-withdrawing PT unit.[4b,12] However, the highest occupied molecular orbital (HOMO) is raised in energy by ∼0.16 eV for **P1** (E_{HOMO} = −5.07 eV) relative to **P3** (E_{HOMO} = −5.23 eV). The slightly raised E_{HOMO} for **P1** and **P2** could be attributed to the more ordered PT orientation, which would improve the HOMO wave function delocalization along the polymer main chain.[13] We recognize that there are inherent problems in determining accurate E_{HOMO} and E_{LUMO} energies from CV measurements.[11] Nonetheless, the electrochemically determined band gaps correlate well with those determined by optical spectroscopy (see SI).

Of primary interest to us was to determine to what degree the backbone structure would impact the charge carrier mobility. Bottom gate, top contact field effect transistors (FETs) with the architecture Si/SiO_2/OTS8/copolymer/Ag were fabricated by spin-casting from 0.5 wt % of polymer solution (*o*-DCB for **P1**, chlorobenzene for **P2** and **P3**; these solvents provide the best performance for each polymer structure) at 2000 rpm for 1 min at room temperature. Note that the high molecular weight samples were used for this purpose. The substrate comprised a highly n-doped silicon wafer with a 200 nm thick SiO_2 gate dielectric treated with octyltrichlorosilane (OTS8). Figure 3 shows the resulting output and transfer $I-V$ characteristics obtained by sweeping the gate bias (V_G) from −60 to 10 V under a source−drain bias (V_D) of −60 V. Both linear and saturation regimes demonstrate p-type-dominated FET behavior. The regioregular polymers exhibited excellent hole mobilities of 0.4 and 0.6 $cm^2\ V^{-1}\ s^{-1}$ for **P1** and **P2**, respectively. Comparatively, the mobility of the regiorandom polymer **P3** was estimated to be 0.005 $cm^2\ V^{-1}\ s^{-1}$, significantly less than that of the regioregular structures. The current on/off ratios (I_{on}/I_{off}) for all FETs are 10^3-10^4. Mobility values and current on/off ratios at room temperature are in Table 1. The ∼2 orders of magnitude increases of hole mobility for **P1** and **P2**, compared to that of the regiorandom copolymer **P3**, indicate the importance of regioregularity for achieving optimal electronic properties. Hole-only diodes (Figure S6) showed a similar trend, where the mobilities of **P1** (1.8×10^{-4} $cm^2\ V^{-1}\ s^{-1}$) and **P2** (2.9×10^{-4} $cm^2\ V^{-1}\ s^{-1}$) are comparable and are 1 order higher than that of **P3** (1.5×10^{-5} $cm^2\ V^{-1}\ s^{-1}$).

Figure 4 shows the surface topography images obtained by atomic force microscopy (AFM) of **P1**, **P2**, and **P3** films used to obtain the best-performing FETs. It was found that all three polymers form smooth films with surface roughness of 2.4, 0.62, and 0.67 nm, respectively. **P1** exhibits connected fiber-like structures with average length of 177 nm and width of 34 nm. The **P2** thin film also shows shorter fibers, with width and length of ∼127 and 45 nm, respectively, and is slightly smoother than **P1**. Even though the roughness of the **P3** film is similar to that of **P2**, ordered structures are observed only in smaller regions of the film. These images show evidence that the regioregular structures provide higher order bulk organization, at least at the surface of the films.

Grazing incident wide-angle X-ray scattering (GIWAXS) measurements of **P1**−**P3** were also carried out to obtain further insight into possible differences of structural order within the bulk (Figure S7).[14] Reflections with strong intensities are observed, which indicate the presence of crystallographic planes with sufficiently large correlation lengths. Distinct differences can be observed for peaks at low q values ($2-6$ nm^{-1}) that report on the separation between the polymer chains as determined by the alkyl side chains.[7] Specifically, in the second-order alkyl reflection region, $q = 4.92$ nm^{-1} for **P1** and **P2** and $q = 5.07$ nm^{-1} for **P3**. Such differences suggest that **P3** forms a crystallite with a different stacking arrangement than **P1** and **P2**. The results are consistent with the idea that backbone regioregularity bears a direct impact on the structural arrangement of the chains.

In summary, two regioregular copolymers built using CDT and PT structural units have been prepared by using

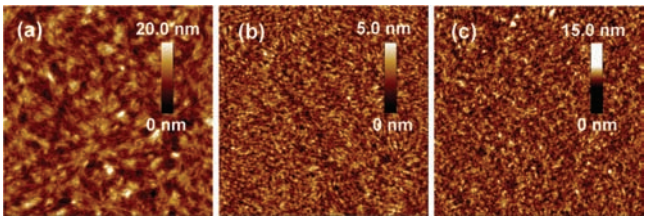

Figure 4. Tapping-mode AFM height images (2 × 2 μm) of **P1** spin-coated from 0.5% *o*-DCB solution (a), **P2** spin-coated from 0.5% chlorobenzene solution (b), and **P3** spin-coated from 0.5% chlorobenzene solution (c) atop a Si/SiO_2/OTS8 substrate.

polymerization reactions involving reactants specifically designed to avoid random orientation of the PT heterocycle. It is also found that the standard polymerizations involving $PTBr_2$ and distannylated CDT reagents yield products with less precise structures. Regioregularity modifies the optical properties and the electronic structure of the materials. More relevant to the design of materials for optoelectronic devices, it is found that the regioregular **P1** and **P2** exhibit much larger hole mobilities, within both FET and diode configurations. These observations are consistent with the higher degree of structural order within the resulting thin films, as indicated by AFM and GIWAXS characterization. We recognize that further structural characterization is required for understanding the exact interchain organization at the dielectric interface in the FET devices, and this is the subject of an ongoing study. From a broader perspective, it is worth highlighting that these guidelines for achieving structurally more precise narrow band materials are relevant within the context of bulk heterojunction polymer solar cells, where balanced charge carrier transport improves power conversion efficiencies.[15]

■ ASSOCIATED CONTENT

Supporting Information. Experimental details and characterization data. This material is available free of charge via the Internet at http://pubs.acs.org.

■ AUTHOR INFORMATION

Corresponding Author
bazan@chem.ucsb.edu

■ ACKNOWLEDGMENT

The authors are grateful to the Mitsubishi Chemical Center for Advanced Materials (MC-CAM) and the Center for Energy Efficient Materials, an Energy Frontier Research Center funded by the U.S. Department of Energy, Office of Science, Office of Basic Energy Sciences under Award No. DE-SC0001009 (support of G.C.W.), for financial support. L.A.P. acknowledges support from the ConvEne IGERT Program (NSF-DGE 0801627) and a Graduate Research Fellowship from the National Science Foundation. Portions of this research were carried out at the Stanford Synchrotron Radiation Lightsource user facility, operated by Stanford University on behalf of the U.S. Department of Energy. W.-Y.W. acknowledges financial support from the Hong Kong Research Grants Council (grant no. HKBU 202410), a grant from Hong Kong Baptist University (FRG2/09-10/091), and the University Grants Committee of HKSAR (AoE/P-03/08).

■ REFERENCES

(1) (a) Günes, S.; Neugebauer, H.; Sariciftci, N. S. *Chem. Rev.* **2007**, *107*, 1324. (b) Thmpson, B. C.; Fréchet, J. M. J. *Angew. Chem., Int. Ed.* **2008**, *47*, 58. (c) Li, Y.; Zou, Y. *Adv. Mater.* **2008**, *20*, 2952. (d) Cheng, Y. J.; Yang, S. H.; Hsu, C. S. *Chem. Rev.* **2009**, *109*, 5868. (e) Li, C.; Liu, M. Y.; Pschirer, N. G.; Baumgarten, M.; Müllen, K. *Chem. Rev.* **2010**, *110*, 6817. (f) Liang, Y. Y.; Yu, L. P. *Acc. Chem. Res.* **2010**, *43*, 1227. (g) Boudreault, P.-L. T.; Najari, A.; Leclerc, M. *Chem. Mater.* **2011**, *23*, 456.

(2) (a) Bijleveld, J. C.; Zoombelt, A. P.; Mathijssen, S. G. J.; Wienk, M. M.; Turbiez, M.; de Leeuw, D. M.; Janssen, R. A. *J. Am. Chem. Soc.* **2009**, *131*, 16616. (b) Wang, M.; Hu, X. W.; Liu, P.; Li, W.; Gong, X.; Huang, F.; Cao, Y. *J. Am. Chem. Soc.* **2011**, *133*, 9638. (c) Li, Y. N.; Sonar, P.; Singh, S. P.; Soh, M. S.; van Meurs, M.; Tan, J. *J. Am. Chem. Soc.* **2011**, *133*, 2198. (d) Yan, H.; Chen, Z. H.; Zheng, Y.; Newman, C.; Quinn, J. R.; Dotz, F.; Kastler, M.; Facchetti, A. *Nature* **2009**, *457*, 679. (e) Zhang, W. M.; Smith, J.; Watkins, S. W.; Gysel, R.; McGehee, M.; Salleo, A.; Kirkpatrick, J.; Ashraf, S.; Anthopoulos, T.; Heeney, M.; McCulloch, I. *J. Am. Chem. Soc.* **2010**, *132*, 11437.

(3) (a) Zhang, M.; Tsao, H. N.; Pisula, W.; Yang, C.; Mishra, A. K.; Müllen, K. *J. Am. Chem. Soc.* **2007**, *129*, 3472. (b) Tsao, H. N.; Cho, D.; Andreasen, J. W.; Rouhanipour, A.; Breiby, D. W.; Pisula, W.; Müllen, K. *Adv. Mater.* **2009**, *21*, 209. (c) Tsao, H. N.; Cho, D. M.; Park, I.; Hansen, M. R.; Mavrinskiy, A.; Yoon, D. Y.; Graf, R.; Pisula, W.; Spiess, H. W.; Müllen, K. *J. Am. Chem. Soc.* **2011**, *133*, 2605.

(4) (a) Blouin, N.; Michaud, A.; Gendron, D.; Wakim, S.; Blair, E.; Neagu-Plesu, R.; Belletête, M.; Durocher, G.; Tao, Y.; Leclerc, M. *J. Am. Chem. Soc.* **2008**, *130*, 732. (b) Zhou, H. X.; Yang, L. Q.; Price., S. C.; Knight, K. J.; You, W. *Angew. Chem., Int. Ed.* **2010**, *49*, 7992. (c) Welch, G. C.; Bazan, G. C. *J. Am. Chem. Soc.* **2011**, *133*, 4632. (d) Steinberger, S.; Mishra, A.; Reinold, E.; Levichkov, J.; Uhrich, C.; Pfeiffer, M.; Bäuerle, P. *Chem. Commun.* **2011**, *47*, 1982. (e) Welch, G. C.; Perez, L. A.; Hoven, C. V.; Zhang, Y.; Dang, X.; Sharenko, A.; Toney, M. F.; Kramer, E. J.; Nguyen, T. Q.; Bazan, G. C. *J. Mater. Chem.* **2011**, *21*, 12700.

(5) (a) Mauer, R.; Kastler, M.; Laquai, F. *Adv. Funct. Mater.* **2010**, *20*, 2085. (b) Guo, J. M.; Ohkita, H.; Benten, H.; Ito, S. *J. Am. Chem. Soc.* **2010**, *132*, 6154. (c) Nambiar, R.; Woody, K. B.; Ochocki, J. D.; Brizius, G. L.; Collard, D. M. *Macromolecules* **2009**, *42*, 43.

(6) (a) Osaka, I.; McCullough, R. D. *Acc. Chem. Res.* **2008**, *41*, 1202. (b) Kim, Y.; Cook, S.; Tuladhar, S. M.; Choulis, S. A.; Nelson, J.; Durrant, J. R.; Bradley, D. D. C.; Giles, M.; McCulloch, I.; Ha, C.-S.; Ree, M. *Nat. Mater.* **2006**, *5*, 197. (c) Woo, C. H.; Thompson, B. C.; Kim, B. J.; Toney, M. F.; Frechet, J. M. J. *J. Am. Chem. Soc.* **2008**, *130*, 16324.

(7) (a) McCulloch, I.; Heeney, M.; Bailey, C.; Genevicius, K.; MacDonald, I.; Shkunov, M.; Sparrowe, D.; Tierney, S.; Wagner, R.; Zhang, W. M.; Chabinyc, M. L.; Kline, R. J.; McGehee, C. D.; Toney, M. F. *Nat. Mater.* **2006**, *5*, 328. (b) Elbing, M.; Garcia, A.; Urban, S.; Nguyen, T. Q.; Bazan, G. C. *Macromolecules* **2008**, *41*, 9146.

(8) (a) Tilley, J. W.; Zawoiski, S. *J. Org. Chem.* **1988**, *53*, 386. (b) Schröter, S.; Stock, C.; Bach, T. *Tetrahedron* **2005**, *61*, 2245. (c) Handy, S. T.; Wilson, T.; Muth, A. *J. Org. Chem.* **2007**, *72*, 8496. (d) Ernst, A.; Gobbi, L.; Vasella, A. *Tetrahedron Lett.* **1996**, *37*, 7959. (e) Lehmann, U.; Henze, O.; Schluter, A. D. *Chem.—Eur. J.* **1999**, *5*, 854.

(9) Park, J. K.; Jo, J.; Seo, J. H.; Moon, J. S.; Park, Y. D.; Lee, K.; Heeger, A. J.; Bazan, G. C. *Adv. Mater.* **2011**, *23*, 2430.

(10) Peet, J.; Cho, N. S.; Lee, S. K.; Bazan, G. C. *Macromolecules* **2008**, *41*, 8655.

(11) Cardona, C. M.; Li, W.; Kaifer, A. E.; Stockdale, D.; Bazan, G. C. *Adv. Mater.* **2011**, *23*, 2367.

(12) (a) Zhou, H. X.; Yang, L. Q.; Xiao, S. Q.; Liu, S. B.; You, W. *Macromolecules* **2010**, *43*, 811. (b) Zheng, Q. D.; Jung, B. J.; Sun, J.; Katz, H. E. *J. Am. Chem. Soc.* **2010**, *132*, 5394.

(13) (a) Tsoi, W. C.; Spencer, S. J.; Yang, L.; Ballantyne, A. M.; Nicholson, P. G.; Turnbull, A.; Shard, A. G.; Murphy, C. E.; Bradley, D. D. C.; Nelson, J.; Kim, J.-S. *Macromolecules* **2011**, *44*, 2944. (b) Mondal, R.; Miyaki, N.; Becerril, H. A.; Norton, J. E.; Parmer, J.; Mayer, A. C.; Tang, M. L.; Brédas, J.-L.; McGehee, M. D.; Bao, Z. N. *Chem. Mater.* **2009**, *21*, 3618.

(14) Rogers, J. T.; Schmidt, K.; Toney, M. F.; Kramer, E. J.; Bazan, G. C. *Adv. Mater.* **2011**, *23*, 2284.

(15) (a) Li, G.; Shrotriya, V.; Huang, J. S.; Yao, Y.; Moriarty, T.; Emery, K.; Yang, Y. *Nat. Mater.* **2005**, *4*, 864. (b) Blom, P. W. M.; Mihailetchi, V.; Koster, L. J. A.; Markov, D. E. *Adv. Mater.* **2007**, *19*, 1551.